

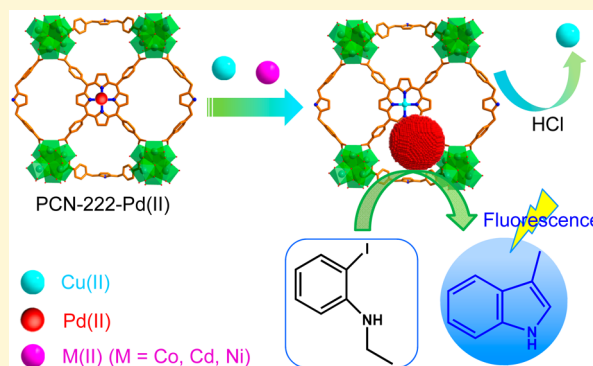
Porphyric Metal–Organic Framework Catalyzed Heck-Reaction: Fluorescence “Turn-On” Sensing of Cu(II) Ion

Yu-Zhen Chen and Hai-Long Jiang*

Hefei National Laboratory for Physical Sciences at the Microscale, CAS Key Laboratory of Soft Matter Chemistry, Collaborative Innovation Center of Suzhou Nano Science and Technology, Department of Chemistry, University of Science and Technology of China, Hefei, Anhui 230026, P.R. China

S Supporting Information

ABSTRACT: It is of great importance for the highly selective, rapid, and sensitive detection of Cu(II) ion, as copper is an essential element in the environment and the human body, and exposure to high concentrations of Cu(II) will potentially cause health issues. In this work, we have developed a novel catalytic Heck reaction system based on Pd(II)-porphyric metal–organic framework (MOF), PCN-222-Pd(II), to generate highly fluorescent product in the presence of Cu(II). In this system, the achieved signal enlargement toward Cu(II) with high sensitivity not only takes advantage of a stronger binding affinity of Cu(II) over Pd(II) to the nitrogen atoms in the porphyrin, but also a rapid Pd(0)-catalyzed Heck-reaction triggered by the addition of Cu(II) ion. Compared with the previous detection methods, the current fluorescence “turn-on” approach not only realizes highly selective and sensitive detection of Cu(II) in aqueous solution, but also is able to separate the Cu(II) from the system. This work would open up a new door for MOF applications in the detection of metal ions in complex environments.



INTRODUCTION

Copper is a ubiquitous metal that plays an important role in environmental and chemical areas. Moreover, as an essential element in biological systems, low concentrations of copper possess the important function for the enzyme activity owing to its redox-active nature.¹ However, it would bring about pollution when too much copper leaks into the environment through multiple ways, and excessive concentrations of copper in the body might cause gastrointestinal disturbance and damage to the liver and kidneys.^{2–7} Particularly, the U.S. Environmental Protection Agency (EPA) has set the limit of copper concentration in drinking water to be 1.3 ppm (~20 μM). Therefore, it is necessary to develop a highly selective and sensitive method for the detection of Cu(II) in aqueous phase.^{8,9}

Several detection techniques for metal ions have been reported, including inductively coupled plasma mass spectrometry (ICP-MS) and inductively coupled plasma atomic emission spectrometry (ICP-AES), and so forth.^{10–12} In addition, quite a few “turn-off” sensors have been developed based on the well-known fluorescent quenching character of Cu(II) ion.^{13–20} However, the “turn-off” sensors are often not as sensitive as the fluorescence enhancement response and hardly used for Cu(II) detection because of the strong hydration ability of Cu(II) in aqueous solution.^{13–16} More recently, many efforts have been dedicated to designing the “turn-on” fluorescent sensors,^{21–29} including excited-state intramolecular proton transfer (ESIPT)-

based reactive probes,^{22,23} catalytic reaction-based probes,^{24–27} DNzyme catalytic beacon sensors,^{9,28} and click chemistry.²⁹ Among them, the catalytic reaction-based signal amplification probes have attracted intense interest, such as Heck-coupling reaction, catalytic hydrolysis of esters, Mannich-Type reaction, C—O bond cleavage reaction-based system, and so forth.^{24–27} It is noteworthy that although most of these methods exhibit sensitive signal response toward Cu(II) ion, they are not suitable for exclusive monitoring of Cu(II) ion in a quantitative fashion in complicated aqueous systems, partially due to the poor water solubility/dispersity of the sensors. Meanwhile, the homogeneous sensors are difficult to remove from the system. Therefore, it is desirable to develop a heterogeneous system for highly selective, sensitive, and quantitative monitoring for Cu(II) ion in aqueous media.

To meet this challenge, the rising crystalline porous materials, metal–organic frameworks (MOFs),^{30–32} could be an alternative solution, given their remarkable features in modular assembly, high surface area, tunability, as well as potential multifunctional applications.^{33–43} A few MOFs have been reported to exhibit sensing behavior for metal ions,^{44–50} almost all of which are based on the fluorescence “turn-off” mechanism with the intrinsic disadvantage mentioned above.

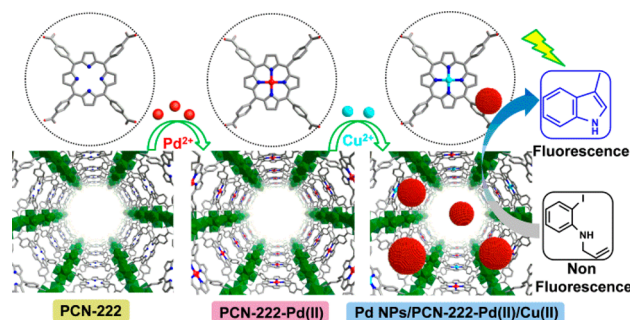
Received: July 24, 2016

Revised: August 27, 2016

Published: August 29, 2016

One major challenge here is to develop a novel MOF system that simultaneously realizes sensitive fluorescence “turn-on” detection and the removal of the metal ions. Recently, Zr-porphyrinic MOFs have attracted escalating interest owing to their unique electronic structures and properties as well as exceptional stability.^{51–60} For example, the PCN-222 (PCN = porous coordination network, also called MOF-545 or MMPF-6) constructed by Zr-oxo clusters and tetrakis(4-carboxyphenyl)porphyrin (TCPP) exhibits ultralarge channels (3.7 nm), high BET surface area (BET, >1600 m²/g), and remarkable stability (pH = 0–9).^{51–54} Remarkably, the involved free-base porphyrin could be inserted into and possesses different affinities to various metal ions, providing potential recognition ability for particular metal ions and thus for sensing function.⁶¹ With these important features, PCN-222 could be an ideal platform as a “turn-on” sensor for Cu(II) detection, involving aniline as a probe molecule, based on the following design: (1) the Pd(II) is preinserted into the porphyrin center to give PCN-222-Pd(II); (2) PCN-222-Pd(II) is highly sensitive to Cu(II), and the Pd(II) is easily replaced by Cu(II) due to a stronger binding affinity between porphyrin and Cu(II) than Pd(II). Simultaneously, the isolated Pd(II), in an equal amount to the inserted Cu(II), would be rapidly reduced in situ to Pd nanoparticles (NPs) stabilized by PCN-222-Pd(II)/Cu(II); (3) the nonfluorescent aniline will be converted to fluorescent ring-closing product via Heck cross-coupling reaction over Pd NPs and thus the Cu(II) detection can be realized based on the difference of fluorescence intensity (Scheme 1). The key point lies in the metal ion exchange from

Scheme 1. Preparation Process from Base-Free PCN-222 to PCN-222-Pd(II) and Finally to Pd NPs/PCN-222-Pd(II)/Cu(II) which Catalyzes Nonfluorescent Aniline to Fluorophore Product via Heck Cross-Coupling Reaction, Realizing Cu(II) Detection and Separation



weakly bonded Pd(II) to strongly bonded Cu(II) in porphyrin centers in PCN-222. In addition, the large channels in PCN-222 would not only facilitate the transportation of Cu(II) and catalytic substrate/product but also favor the stabilization/confinement of Pd NPs. To the best of our knowledge, this is the first work demonstrating metalloporphyrin-based MOFs for catalytic signal amplification, which is used in highly selective fluorescence chemosensors for trace amounts of Cu(II) ion and performs a very low detection limitation in reference to those reported MOF sensors.

EXPERIMENTAL SECTION

Materials and Instrumentation. All commercial chemicals were used without further purification unless stated otherwise. Powder X-ray diffraction patterns (XRD) were carried out on either a Japan Rigaku SmartLab rotation anode X-ray diffractometer or a Holland

X'Pert PRO fixed anode X-ray diffractometer equipped with graphite monochromatized Cu K α radiation ($\lambda = 1.54178 \text{ \AA}$). Fluorescent emission spectra were conducted on a LS-55 fluorescent spectrometer made by PerkinElmer. The UV–vis absorption spectra were recorded on a UV–vis spectrophotometer (TU-1810, Beijing Pgeneral, China) in the wavelength range of 200–800 nm. The contents of Pd and Cu species in the samples were quantified by an Optima 7300 DV inductively coupled plasma atomic emission spectrometer (ICP-AES). Field-emission scanning electron microscopy (FE-SEM) was carried out with a field emission scanning electron microanalyzer (Zeiss Supra 40 scanning electron microscope at an acceleration voltage of 5 kV). The size, morphology, and microstructure of Pd NPs/PCN-222-Pd(II)/Cu(II) were investigated using transmission electron microscopy (TEM) on JEOL-2010 with an electron acceleration energy of 200 kV. The nitrogen sorption isotherms were measured using automatic volumetric adsorption equipment (Micromeritics ASAP 2020). Prior to nitrogen adsorption/desorption measurements, the as-synthesized samples were activated in DMF with 2 M HCl and then subsequently washed sufficiently with DMF and acetone. Then the solid was left to soak in acetone for a certain time. Following that, the sample was dried in vacuum at 50 °C for 12 h and then 120 °C overnight. The ¹H NMR was recorded on a Bruker AC-400 FT (400 MHz) using TMS as internal reference. Catalytic reaction products were analyzed and identified by gas chromatography (GC, Shimadzu 2010Plus with a 0.25 mm \times 30 m Rtx-5 capillary column).

Preparation of Ligand. The tetrakis(4-carboxyphenyl)porphyrin (H₂TCPP) was prepared according to procedures described in previous report.⁵¹ Typically, pyrrole (6.0 g, 0.086 mol), methyl *p*-formylbenzoate (14 g, 0.084 mol) and propionic acid (200 mL) were mixed in a 500 mL three-necked flask. Then the solution was refluxed at 140 °C overnight. After cooling to room temperature, the purple solid was filtrated, followed by thorough washing with ethanol, ethyl acetate, and THF, and finally drying in vacuum at 60 °C. The obtained ester (6 g) was dissolved in a mixed solvent of THF (100 mL) and MeOH (100 mL), and then KOH (21 g, 375.6 mmol) in H₂O (100 mL) was introduced. This mixture was refluxed for 12 h. After being cooled down to room temperature, the organic solvents were evaporated. Additional water was added to the resulting mixture to give a homogeneous solution, followed by acidification with 1 M HCl until no further precipitate was produced. Finally, the purple solid was collected by filtration, washed with water, and dried in vacuum at 60 °C.

Preparation of PCN-222. The PCN-222 was prepared according to the documented method.⁵¹ Typically, ZrCl₄ (70 mg), TCPP (50 mg), and benzoic acid (2.7 g) in 8 mL of DEF were ultrasonically dissolved in a 20 mL high-pressure autoclave. The mixture was first heated in a 120 °C oven for 48 h and then in a 130 °C oven for another 12 h. After being cooled down to room temperature, dark brown needle shaped crystals were harvested by filtration.

Preparation of *N*-Allyl-2-iodoaniline. The allyl bromide (3.0 mmol, 100 μ L) was slowly and dropwise added into a solution of 2-iodoaniline (2.5 mmol, 547.6 mg) and potassium carbonate (1.0 equiv) in DMF (15 mL). Then, the reaction mixture was allowed to stir at room temperature for 16 h. Finally, the reaction mixture was extracted with ethyl acetate (15 mL) for at least three times. The organic layer was dried with MgSO₄ and then filtered and evaporated, followed by silica gel column chromatography (EtOAc/hexane, 1/20) to afford pure *N*-allyl-2-iodoaniline (yield, 80%).

General Procedures for the Heck Cross-Coupling Reaction over Different Catalytic Systems. With PCN-222-Pd(II) in Absence or Presence of Cu(II). A 20 mL mixture of acetonitrile and water (V:V = 10:1) in a 25 mL three-neck, round-bottom flask was deoxygenated by bubbling nitrogen for at least 1 h, followed by the addition of activated PCN-222 (containing 0.025 mM porphyrin unit), and the mixture was sonicated for around 20 min until it became homogeneous. After bubbling nitrogen for 1 h, palladium acetate solution with the desired concentration (0.025 mM) was added dropwise over a period of 10 min during constant vigorous stirring. Then the resultant mixture was stirred at 60 °C under nitrogen

atmosphere for 1 h to afford PCN-222-Pd(II). The *N*-allyl-2-iodoaniline (0.5 mM), tri(*o*-tolyl)phosphine (cocatalyst, 0.05 mM), and TEA (1 mM) were added into the above mixture solution under nitrogen, and the reactant system was bubbled with nitrogen for another 1 h. The reaction started when a series of copper acetate solutions with various concentrations (0.05–2 μ M) was added into the flask. The emission spectra were taken every 10 min to track the reaction process. The fluorescent product was excited at 275 nm, and the emission at 351 nm was monitored.

With PCN-222-Cu(II) in Absence or Presence of Pd(II). A 20 mL mixture of acetonitrile and water (V:V = 10:1) in a 25 mL three-neck round-bottom flask was deoxygenated by bubbling nitrogen for at least 1 h. Followed by the addition of activated PCN-222 (containing 0.025 mM porphyrin unit), the mixture was sonicated for around 20 min until it became homogeneous. After bubbling nitrogen for 1 h, copper(II) acetate solution (0.025 mM) was added dropwise over a period of 10 min during constant vigorous stirring to afford PCN-222-Cu(II). Then, *N*-allyl-2-iodoaniline (0.5 mM), tri(*o*-tolyl)phosphine (0.05 mM), and TEA (1 mM) were added into the above mixture solution, and the reactant system was bubbled with nitrogen for another 1 h. The reaction started when palladium acetate (0.025 μ M) was added into the flask. The emission spectra were taken every 10 min to track the reaction process.

With H₂-TCPP. A 20 mL mixture of acetonitrile and water (V:V = 10:1) in a 25 mL three-neck round-bottom flask was deoxygenated by bubbling nitrogen for at least 1 h. Followed by the addition of activated H₂-TCPP (containing 0.025 mM porphyrin unit), the mixture was sonicated for around 20 min until it became homogeneous. After bubbling nitrogen for 1 h, palladium acetate solution with the desired concentration was added dropwise over a period of 10 min during constant vigorous stirring. Then the resultant mixture was stirred at 60 °C under nitrogen atmosphere for 1 h to give Pd(II)-TCPP. The *N*-allyl-2-iodoaniline (0.5 mM), tri(*o*-tolyl)phosphine (0.05 mM), and TEA (1 mM) were added into above mixture solution under nitrogen, and the reactant system was bubbled with nitrogen for another 1 h. The reaction started when copper acetate solution (0.25 μ M) was added into the flask. The emission spectra were taken every 10 min to track the reaction process.

RESULTS AND DISCUSSION

The PCN-222 with free-base porphyrin in needle shape (Figure S1 of the Supporting Information) was synthesized according to the documented method.⁵¹ The high N₂ adsorption and surface area (1611 m²/g) demonstrate the highly porous structure of PCN-222 (Figure S2). The porphyrin unit involved in PCN-222 is able to capture metal ions under certain conditions. Therefore, the Pd(II) with an equivalent amount of porphyrin was used to chelate with the porphyrin N atoms to form PCN-222-Pd(II), which then acts as a highly selective probe for Cu(II) ion in aqueous solution. The Heck cross-coupling reaction between *N*-allyl-2-iodoaniline and allyl bromide has been chosen for the detection because of the completely different fluorescent properties between reactants (nonfluorescent) and product (3-methylindole, fluorescent), as previously reported.²⁴ The fluorescence of the product, tracking the reaction progress, can be simply monitored by fluorescent emission spectrum during the catalytic reaction.

The as-synthesized *N*-allyl-2-iodoaniline (0.5 mM, identified by ¹H NMR, Figure S3), tri(*o*-tolyl)phosphine (0.05 mM), and triethylamine (TEA, 1 mM) were added into the acetonitrile–water solution with PCN-222 (containing 0.025 mM porphyrin unit) under nitrogen. After bubbling the reaction system with nitrogen, the reaction started after copper acetate solutions with different concentrations (0.05–2 μ M) were introduced. Each equivalent of Cu(II) will free up the same amount of Pd(II) to be reduced to Pd NPs, producing Pd NPs/PCN-222-Pd(II)/

Cu(II) for catalyzing the Heck coupling reaction. As a result, the nonfluorescent aniline was quickly converted to the fluorescent indole product, and the fluorescence was catalytically “turned-on”. The solution was excited at 280 nm (absorption maximum), and the emission at 351 nm was monitored for the indole product (Figure 1). The fluorescence emission spectra were recorded every 10 min to track the reaction process.

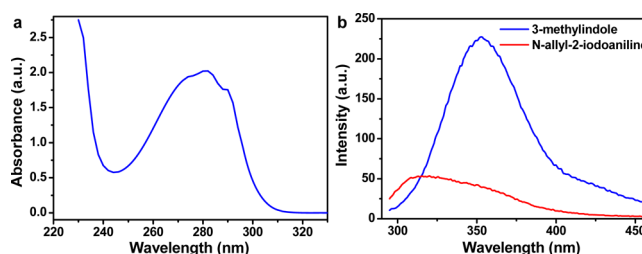


Figure 1. (a) Absorption spectrum of the product 3-methylindole. (b) Emission spectra of the reactant (*N*-allyl-2-iodoaniline) and product (3-methylindole). The solution was excited at 280 nm.

As displayed in Figure 2a, the fluorescence intensity of the mixture solution in the presence of 0.25 μ M Cu(II) persistently

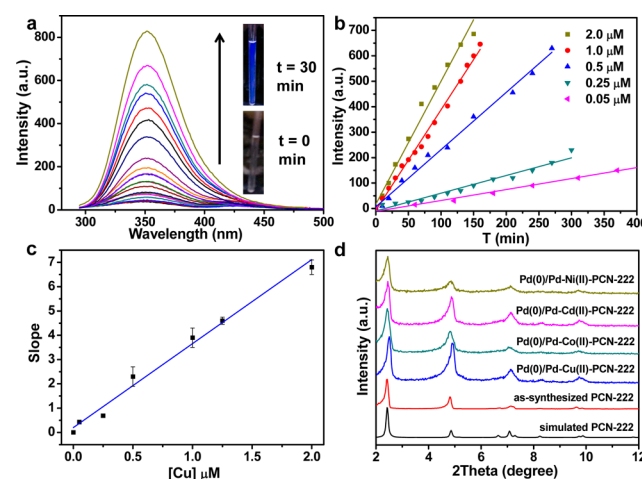


Figure 2. (a) The fluorescence spectra of the solution during the Heck reaction (0.25 μ M Cu(II)) as a representative; inset: the optical photographs for the reaction solution before and after the catalytic reaction under UV light irradiation. (b) The relationship between the fluorescence intensity of the solution vs time, reflecting the initial reaction rate toward various concentrations of Cu(II). (c) Slope (initial rate) vs the concentration of Cu(II) ranging from 2000 to 50 nM. (d) Powder XRD patterns for simulated PCN-222 and experimental PCN-222-based catalysts after sensing of different metal ions. Reaction conditions: PCN-222 (involving 0.025 mM porphyrin), *N*-allyl-2-iodoaniline (0.025 mM), tri(*o*-tolyl)phosphine (0.05 mM), TEA (1 mM), CH₃CN/H₂O (10/1), 60 °C, and N₂ bubbling.

increases along with the generation of fluorescent product during the reaction process. Similarly, the fluorescence intensity of the solution with other Cu(II) concentrations also increases along with reaction time (Figure S4). Accordingly, the original colorless solution becomes blue under UV light irradiation (Figure 2a, inset). Figure 2b indicates the relationship between the fluorescence intensity and time, with various concentrations of Cu(II) introduced into the reaction solution. As expected,

along with the decreasing Cu(II) concentration introduced, the slopes of the curves that represent initial rate kinetics gradually decreases. Strikingly, the detection limit based on PCN-222-Pd(II) for Cu(II) is able to reach 50 nM, which is far below the limit of copper in drinking water that required by U.S. EPA ($\sim 20 \mu\text{M}$) and almost all previously reported MOF sensors for metal ion (Table S1).^{44–50} Furthermore, there almost exists a linear relationship between the slope and Cu(II) concentration (Figure 2c), indicating that 1 equiv of Cu(II) frees up the same amount of Pd(II). In light of this result, the PCN-222-Pd(II) could be used as a standard reference material for Cu(II) detection in environmental and industrial wastewater. Remarkably, the resultant catalyst containing Cu(II) is readily separated from the reaction system via simple centrifugation. In contrast, the previously reported Cu(II) fluorescent sensor (PAC-Pd(II)) is hard to be separated from the homogeneous system.²⁴ The powder X-ray diffraction (XRD) profiles for Pd NPs/PCN-222-Pd(II)/Cu(II), in which $0.25 \mu\text{M}$ Cu(II) as a representative hereafter unless otherwise specified, demonstrate the retained crystallinity and structural integrity of the PCN-222 framework (Figure 2d). Nitrogen sorption at 77 K shows the of PCN-222 is mostly maintained in the obtained Pd NPs/PCN-222-Pd(II)/Cu(II) catalyst, the BET surface area of which is $1190 \text{ m}^2/\text{g}$ (Figure S5). The decrease of the surface area could be attributed to the mass contribution of the additional Cu(II) and the partial blocking of the MOF pores by the Pd NPs, which is in agreement with previous reports.^{62–68} The transmission electron microscopy (TEM) observation for Pd NPs/PCN-222-Pd(II)/Cu(II) shows the generation of uniformly dispersed Pd NPs with average size of $\sim 3.6 \text{ nm}$ (Figure S6). The powder XRD pattern of Pd NPs/PCN-222-Pd(II)/Cu(II) in a wide range presents the signal of Pd(0) species, further reflecting the presence of crystalline Pd NPs (Figure S7). X-ray photoelectron spectroscopy (XPS) spectrum for Pd NPs/PCN-222-Pd(II)/Cu(II) demonstrates the presence of C, Cu, Pd, O, and N (Figure S8a). The metallic Pd species can be clearly identified by the binding energies at 336.07 and 341.33 eV, respectively, assignable to Pd $3d_{5/2}$ and $3d_{3/2}$, and the shoulder peaks at 338.09 and 343.34 eV can be related to the $3d_{5/2}$ and $3d_{3/2}$ levels of Pd(II), respectively (Figure S8c), implying that only a part of the Pd(II) cations were reduced to Pd(0). The very weak peak at 933.4 eV for Cu(II) $2p_{3/2}$ suggests the low content of Cu species (Figure S8d). Inductively coupled plasma atomic emission spectrometry (ICP-AES) has confirmed that the actual contents of Pd (8.11 wt %) and Cu (2.19 wt %) in Pd NPs/PCN-222-Pd(II)/Cu(II) (with $9 \mu\text{M}$ Cu as a representative) are very close to the nominal values (8 wt % for Pd and 1.92 wt % for Cu). Interestingly, the Cu(II) ion tightly bound in the porphyrin center can be completely released from the catalyst after being treated with 6 M HCl solution, as evidenced by the ICP-AES analysis. Therefore, different from all previous reports (especially for the PAC-Pd(II)²⁴), the current sensor approach we designed not only successfully detects the Cu(II) ions, but also is able to separate the Cu(II) ions from the system. On the basis of above results, the successful detection with high sensitivity and selectivity toward Cu(II) can be attributed to the following aspects: (1) the stronger binding affinity of Cu(II) than Pd(II) to the porphyrin; (2) the introduction of Cu(II) results in an equal amount of Pd(II) being reduced in situ to Pd NPs stabilized by PCN-222, which catalyzes the Heck reaction; (3) the distinctly different fluorescence properties of the reactant and product facilitate the monitoring of the catalytic

reaction; and (4) the slopes of the lines (fluorescence intensity vs time) that represent the reaction rates are directly associated with the Cu(II) concentrations.

To better elucidate the Cu(II) detection based on PCN-222-Pd(II), several sets of control experiments have been carried out under similar conditions. It is found that the catalytic Heck-coupling reaction does not occur in the absence of Cu(II). The result not only implies that all Pd(II) ions are linked with porphyrin rings and no free Pd(II) ion exists in the system, but also demonstrates that Pd(II) is not active for the Heck coupling reaction. When the porphyrin was first premetallated with Cu(II) to afford PCN-222-Cu(II), no fluorescence signal can be detected without the addition of Pd(II). In sharp contrast, the reaction starts immediately once Pd(II) is added into the reaction system, and the rate becomes very fast, indicating that the Cu species has no catalytic ability, while the Pd(II) ions, with high redox potential ($E_{\text{Pd}^{2+}/\text{Pd}}^{\circ} = +0.987 \text{ eV}$ vs SHE), can be readily reduced by the weak reductant, triethylamine (TEA). Notably, when PCN-222 is replaced by the homogeneous TCPP linker, the Heck reaction exhibits a slower initial rate under identical conditions, possibly due to the aggregation of the generated Pd NPs in such a homogeneous system in the absence of a pore confinement effect from porous materials, like PCN-222, which has been demonstrated by the TEM observation and size distribution of Pd NPs (Figure S9).

Given the good affinity of transition metal ions to the porphyrin center, we set out to investigate the selectivity of the current sensing protocol for other similar metal ions, such as, Co(II), Ni(II), Cd(II), and so forth. It is assumed that the Pd(II) in the porphyrin center can also be displaced by these metal ions. The experimental results unambiguously show the inferior sensing ability toward other metal ions and the best selectivity toward Cu^{2+} among all these M(II) ions (Figure 3a). Compared to the almost constant slope for Cu(II), the slopes for all other metal ions are obviously divided into two segments, in which the slope in the first section (0–150 min) is much smaller than that in the subsequent one (after 150 min). Remarkably, the initial slope of Cu(II) is almost 5-fold, 7-fold, and 10-fold that for Co(II), Ni(II), and Cd(II), respectively. The distinct difference among initial slopes for different M(II) ions (Figure 3b), reflecting the reaction rate, could be attributed to the much stronger affinity of Cu(II) to porphyrin centers in PCN-222 than that in other metal ions. Therefore, compared to Cu(II), other metal ions free up Pd(II) from the porphyrin center in a very slow initial rate, that is, a very slow sensing rate. As a result, the PCN-222-Pd(II) is able to identify and differentiate Cu(II) from various M(II) mixtures.

CONCLUSIONS

In summary, we have developed a novel signal amplification strategy based on a catalytic reaction over porphyrinic MOF, PCN-222-Pd(II), as a fluorescent “turn-on” sensor, which manifests strong fluorescence enhancement response in the presence of Cu(II) ion and a very sensitive sensing technique. The successful detection of Cu(II) with high sensitivity (up to 50 nM) and selectivity (over other transition metal ions) can be ascribed to the following aspects: (1) the strong binding affinity of Cu(II) to the porphyrin center results in quick liberation of Pd(II) in PCN-222-Pd(II); (2) the unbound Pd(II) ion, in an equal amount of Cu(II) introduced, is rapidly reduced by TEA to Pd NPs stabilized by PCN-222; (3) the generated Pd NPs

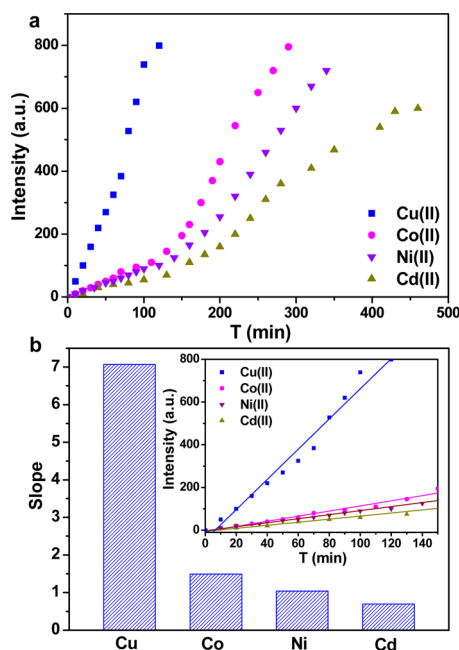


Figure 3. (a) The fluorescence intensity of the catalytic reaction product by introducing different metal ions, including Cu(II), Co(II), Ni(II), and Cd(II). (b) The slope (initial reaction rate) vs the different M(II) (M = Cu, Co, Ni, Cd) (inset: the initial fluorescence intensity vs reaction time for various metal ions). Reaction conditions: PCN-222 (0.5 mM porphyrin), [M(II)] = 9 μ M, *N*-allyl-2-iodoaniline (0.5 mM), tri(*o*-tolyl)phosphine (0.05 mM), TEA (1 mM), CH₃CN/H₂O (10/1), 60 °C, and N₂ bubbling.

are very active for Heck-coupling reaction, which converts the nonfluorescent reactants to the fluorescent indole product, creating visualization; and (4) the slope (fluorescence intensity vs time) represents the reaction rate, in line with the concentration of Cu(II) introduced. Given the significantly higher affinity of Cu(II) to porphyrin, the PCN-222-Pd(II) sensor possesses much higher selectivity toward Cu(II) than Co(II), Ni(II), and Cd(II), etc. Moreover, it is facile to separate the sensor from the system and free up Cu(II) ion by simple treatment with HCl, which would be very attractive in large-scale detection and excessive Cu(II) recovery and exhibits additional advantage compared to the homogeneous sensors. The MOF-based “turn-on” sensor for highly sensitive and selective detection, although in a premature stage, will not only open up new opportunities for MOF applications, but also presents a promising future for practical detection of metal ions.

■ ASSOCIATED CONTENT

Supporting Information

The Supporting Information is available free of charge on the ACS Publications website at DOI: 10.1021/acs.chemmater.6b03030.

Additional characterization data. Experimental details including materials, sample preparation, characterization, and device fabrication and measurements (PDF)

■ AUTHOR INFORMATION

Corresponding Author

*E-mail: jianglab@ustc.edu.cn (H.-L.J.).

Notes

The authors declare no competing financial interest.

■ ACKNOWLEDGMENTS

This work was supported by the NSFC (21371162, 51301159, and 21521001), the 973 program (2014CB931803), the NSF of Anhui Province (1408085MB23), the Recruitment Program of Global Youth Experts, and the Fundamental Research Funds for the Central Universities (WK2060190026, WK2060190065).

■ REFERENCES

- (1) Krämer, R. Fluorescent Chemosensors for Cu²⁺ Ions: Fast, Selective, and Highly Sensitive. *Angew. Chem., Int. Ed.* **1998**, *37*, 772–773.
- (2) Zietz, B. P.; de Vergara, J. D.; Dunkelberg, H. Copper Concentrations in Tap Water and Possible Effects on Infant's Health-Results of A study in Lower Saxony, Germany. *Environ. Res.* **2003**, *92*, 129–138.
- (3) Barranguet, C.; van den Ende, F. P.; Rutgers, M.; Breure, A. M.; Greijdanus, M.; Sinke, J. J.; Admiraal, W. Copper-Induced Modifications of the Trophic Relations in Riverine Algal-bacterial Biofilms. *Environ. Toxicol. Chem.* **2003**, *22*, 1340–1349.
- (4) Sivaraman, G.; Anand, T.; Chellappa, D. Quick Accessible Dual Mode Turn-on Red Fluorescent Chemosensor for Cu(II) and Its Applicability in Live Cell Imaging. *RSC Adv.* **2013**, *3*, 17029–17033.
- (5) Tharmaraj, V.; Pitchumani, K. A Highly Selective Ratiometric Fluorescent Chemosensor for Cu(II) Based on Dansyl-functionalized Thiol Stabilized Silver Nanoparticles. *J. Mater. Chem. B* **2013**, *1*, 1962–1967.
- (6) Ponniah, S. J.; Barik, S. K.; Thakur, A.; Ganesamoorthi, R.; Ghosh, S. Triazolyl Alkoxy Fischer Carbene Complexes in Conjugation with Ferrocene/Pyrene as Sensory Units: Multifunctional Chemosensors for Lead(II), Copper(II), and Zinc(II) Ions. *Organometallics* **2014**, *33*, 3096–3107.
- (7) Thakur, A.; Mandal, D.; Deb, P.; Mondal, B.; Ghosh, S. Synthesis of Triazole Linked Fluorescent Amino Acid and Carbohydrate Bioconjugates: A Highly Sensitive and Skeleton Selective Multi-responsive Chemosensor for Cu(II) and Pb(II)/Hg(II) Ions. *RSC Adv.* **2014**, *4*, 1918–1928.
- (8) Royzen, M.; Dai, Z.; Canary, J. W. Ratiometric Displacement Approach to Cu(II) Sensing by Fluorescence. *J. Am. Chem. Soc.* **2005**, *127*, 1612–1613.
- (9) Liu, J.; Lu, Y. A DNAzyme Catalytic Beacon Sensor for Paramagnetic Cu²⁺ Ions in Aqueous Solution with High Sensitivity and Selectivity. *J. Am. Chem. Soc.* **2007**, *129*, 9838–9839.
- (10) Liu, Y.; Liang, P.; Guo, L. Nanometer Titanium Dioxide Immobilized on Silica Gel as Sorbent for Preconcentration of Metal Ions Prior to Their Determination by Inductively Coupled Plasma Atomic Emission Spectrometry. *Talanta* **2005**, *68*, 25–30.
- (11) Li, Y.; Chen, C.; Li, B.; Sun, J.; Wang, J.; Gao, Y.; Zhao, Y.; Chai, Z. J. Elimination Efficiency of Different Reagents for The Memory Effect of Mercury Using ICP-MS. *J. Anal. At. Spectrom.* **2006**, *21*, 94–96.
- (12) Gonzales, A. P. S.; Firmino, M. A.; Nomura, C. S.; Rocha, F. R. P.; Oliveira, P. V.; Gaubeur, I. Peat as A Natural Solid-Phase for Copper Preconcentration and Determination in a Multicommuted Flow System Coupled to Flame Atomic Absorption Spectrometry. *Anal. Chim. Acta* **2009**, *636*, 198–204.
- (13) Tang, B.; Niu, J.; Yu, C.; Zhuo, L.; Ge, J. Highly Luminescent Water-Soluble CdTe Nanowires as Fluorescent Probe to Detect Copper(II). *Chem. Commun.* **2005**, *33*, 4184–4186.
- (14) Jung, H. S.; Kwon, P. S.; Lee, J. W.; Kim, J. I.; Hong, C. S.; Kim, J. W.; Yan, S.; Lee, J. Y.; Lee, J. H.; Joo, T.; Kim, J. S. Coumarin-Derived Cu²⁺-Selective Fluorescence Sensor: Synthesis, Mechanisms, and Applications in Living Cells. *J. Am. Chem. Soc.* **2009**, *131*, 2008–2012.
- (15) Xiao, Y.; Cui, Y.; Zheng, Q.; Xiang, S.; Qian, G.; Chen, B. A Microporous Luminescent Metal-Organic Framework for Highly Selective and Sensitive Sensing of Cu²⁺ in Aqueous Solution. *Chem. Commun.* **2010**, *46*, 5503–5505.

- (16) You, Y.; Han, Y.; Lee, Y.-M.; Park, S. Y.; Nam, W.; Lippard, S. J. Phosphorescent Sensor for Robust Quantification of Copper(II) Ion. *J. Am. Chem. Soc.* **2011**, *133*, 11488–11491.
- (17) Carter, K. P.; Young, A. M.; Palmer, A. E. Fluorescent Sensors for Measuring Metal Ions in Living Systems. *Chem. Rev.* **2014**, *114*, 4564–4601.
- (18) Aron, A. T.; Ramos-Torres, K. M.; Cotruvo, J. A., Jr.; Chang, C. J. Recognition- and Reactivity-Based Fluorescent Probes for Studying Transition Metal Signaling in Living Systems. *Acc. Chem. Res.* **2015**, *48*, 2434–2442.
- (19) Han, Y.; Ding, C.; Zhou, J.; Tian, Y. Single Probe for Imaging and Biosensing of pH, Cu²⁺ Ions, and pH/Cu²⁺ in Live Cells with Ratiometric Fluorescence Signals. *Anal. Chem.* **2015**, *87*, 5333–5339.
- (20) Lei, C.; Wang, Z.; Nie, Z.; Deng, H.; Hu, H.; Huang, Y.; Yao, S. Resurfaced Fluorescent Protein as a Sensing Platform for Label-Free Detection of Copper(II) Ion and Acetylcholinesterase Activity. *Anal. Chem.* **2015**, *87*, 1974–1980.
- (21) Sivaraman, G.; Anand, T.; Chellappa, D. A Fluorescence Switch for the Detection of Nitric Oxide and Histidine and Its Application in Live Cell Imaging. *ChemPlusChem* **2014**, *79*, 1761–1766.
- (22) Ghosh, P.; Bharadwaj, P. K.; Roy, J.; Ghosh, S. Transition Metal (II)/(III), Eu(III), and Tb(III) Ions Induced Molecular Photonic OR Gates Using Trianthryl Cryptands of Varying Cavity Dimension. *J. Am. Chem. Soc.* **1997**, *119*, 11903–11909.
- (23) Kaur, S.; Kumar, S. Photoactive Chemosensors 3: A Unique Case of Fluorescence Enhancement with Cu(II). *Chem. Commun.* **2002**, 2840–2841.
- (24) Wu, Q.; Anslyn, E. V. Catalytic Signal Amplification Using a Heck Reaction. An Example in the Fluorescence Sensing of Cu(II). *J. Am. Chem. Soc.* **2004**, *126*, 14682–14683.
- (25) Wen, Z.-C.; Yang, R.; He, H.; Jiang, Y.-B. A Highly Selective Charge Transfer Fluoroionophore for Cu²⁺. *Chem. Commun.* **2006**, 47, 106–108.
- (26) Guo, H.-M.; Minakawa, M.; Tanaka, F. Fluorogenic Imines for Fluorescent Detection of Mannich-Type Reactions of Phenols in Water. *J. Org. Chem.* **2008**, *73*, 3964–3966.
- (27) Taki, M.; Iyoshi, S.; Ojida, A.; Hamachi, I.; Yamamoto, Y. Development of Highly Sensitive Fluorescent Probes for Detection of Intracellular Copper(I) in Living Systems. *J. Am. Chem. Soc.* **2010**, *132*, 5938–5939.
- (28) Su, Y.-T.; Lan, G.-Y.; Chen, W.-Y.; Chang, H.-T. Detection of Copper Ions Through Recovery of the Fluorescence of DNA-Templated Copper/Silver Nanoclusters in the Presence of Mercaptopropionic Acid. *Anal. Chem.* **2010**, *82*, 8566–8572.
- (29) Ge, C.; Luo, Q.; Wang, D.; Zhao, S.; Liang, X.; Yu, L.; Xing, X.; Zeng, L. Colorimetric Detection of Copper(II) Ion Using Click Chemistry and Hemin/G-Quadruplex Horseradish Peroxidase-Mimicking DNzyme. *Anal. Chem.* **2014**, *86*, 6387–6392.
- (30) Long, J. R.; Yaghi, O. M. The Pervasive Chemistry of Metal–Organic Frameworks. *Chem. Soc. Rev.* **2009**, *38*, 1213–1214.
- (31) Zhou, H.-C.; Long, J. R.; Yaghi, O. M. Introduction to Metal–Organic Frameworks. *Chem. Rev.* **2012**, *112*, 673–674.
- (32) Zhou, H.-C.; Kitagawa, S. Metal–Organic Frameworks (MOFs). *Chem. Soc. Rev.* **2014**, *43*, 5415–5418.
- (33) Liu, Y.; Tang, Z. Multifunctional Nanoparticle@MOF Core–Shell Nanostructures. *Adv. Mater.* **2013**, *25*, 5819–5825.
- (34) Gascon, J.; Corma, A.; Kapteijn, F.; Llabrés i Xamena, F. X. Metal Organic Framework Catalysis: *Quo vadis?* *ACS Catal.* **2014**, *4*, 361–378.
- (35) Zhang, T.; Lin, W. Metal–Organic Frameworks for Artificial Photosynthesis and Photocatalysis. *Chem. Soc. Rev.* **2014**, *43*, 5982–5993.
- (36) Chen, B.; Xiang, S.; Qian, G. Metal–Organic Frameworks with Functional Pores for Recognition of Small Molecules. *Acc. Chem. Res.* **2010**, *43*, 1115–1124.
- (37) Kreno, L. E.; Leong, K.; Farha, O. K.; Allendorf, M.; Van Duyne, R. P.; Hupp, J. T. Metal–Organic Framework Materials as Chemical Sensors. *Chem. Rev.* **2012**, *112*, 1105–1125.
- (38) Mallick, A.; Garai, B.; Díaz, D. D.; Banerjee, R. Hydrolytic Conversion of a Metal–Organic Polyhedron into a Metal–Organic Framework. *Angew. Chem., Int. Ed.* **2013**, *52*, 13755–13759.
- (39) Lin, R.-B.; Li, F.; Liu, S.-Y.; Qi, X.-L.; Zhang, J.-P.; Chen, X.-M. A Noble-Metal-Free Porous Coordination Framework with Exceptional Sensing Efficiency for Oxygen. *Angew. Chem., Int. Ed.* **2013**, *52*, 13429–13433.
- (40) Wang, Z.; Cohen, S. M. Postsynthetic Modification of Metal–Organic Frameworks. *Chem. Soc. Rev.* **2009**, *38*, 1315–1329.
- (41) Hu, Z.; Zhang, K.; Zhang, M.; Guo, Z.; Jiang, J.; Zhao, D. A Combinatorial Approach towards Water-Stable Metal–Organic Frameworks for Highly Efficient Carbon Dioxide Separation. *ChemSusChem* **2014**, *7*, 2791–2795.
- (42) Faustini, M.; Kim, J.; Jeong, G.-Y.; Kim, J. Y.; Moon, H. R.; Ahn, W.-S.; Kim, D.-P. Microfluidic Approach toward Continuous and Ultrafast Synthesis of Metal–Organic Framework Crystals and Hetero Structures in Confined Microdroplets. *J. Am. Chem. Soc.* **2013**, *135*, 14619–14626.
- (43) Tang, Y.-J.; Gao, M.-R.; Liu, C.-H.; Li, S.-L.; Jiang, H.-L.; Lan, Y.-Q.; Han, M.; Yu, S.-H. Porous Molybdenum-Based Hybrid Catalysts for Highly Efficient Hydrogen Evolution. *Angew. Chem., Int. Ed.* **2015**, *54*, 12928–12932.
- (44) Chen, B.; Wang, L.; Xiao, Y.; Fronczek, F. R.; Xue, M.; Cui, Y.; Qian, G. A Luminescent Metal–Organic Framework with Lewis Basic Pyridyl Sites for the Sensing of Metal Ions. *Angew. Chem., Int. Ed.* **2009**, *48*, 500–503.
- (45) Hao, Z. M.; Song, X. Z.; Zhu, M.; Meng, X.; Zhao, S. N.; Su, S. Q.; Yang, W. T.; Song, S. Y.; Zhang, H. J. One-Dimensional Channel-Structured Eu-MOF for Sensing Small Organic Molecules and Cu²⁺ Ion. *J. Mater. Chem. A* **2013**, *1*, 11043–11050.
- (46) Bhattacharyya, S.; Chakraborty, A.; Jayaramulu, K.; Hazra, A.; Maji, T. K. A Bimodal Anionic MOF: Turn-Off Sensing of Cu^{II} and Specific Sensitization of Eu^{III}. *Chem. Commun.* **2014**, *50*, 13567–13570.
- (47) Ye, J.; Zhao, L.; Bogale, R. F.; Gao, Y.; Wang, X.; Qian, X.; Guo, S.; Zhao, J.; Ning, G. Highly Selective Detection of 2,4,6-Trinitrophenol and Cu²⁺ Ions Based on a Fluorescent Cadmium–Pamoate Metal–Organic Framework. *Chem. - Eur. J.* **2015**, *21*, 2029–2037.
- (48) Qiao, C.; Qu, X.; Yang, Q.; Wei, Q.; Xie, G.; Chen, S.; Yang, D. Instant High-Selectivity Cd-MOF Chemosensor for Naked-Eye Detection of Cu(II) Confirmed Using *In Situ* Microcalorimetry. *Green Chem.* **2016**, *18*, 951–956.
- (49) Liu, B.; Wu, W.-P.; Hou, L.; Wang, Y.-Y. Four Uncommon Nanocage-Based Ln-MOFs: Highly Selective Luminescent Sensing for Cu²⁺ Ions and Selective CO₂ Capture. *Chem. Commun.* **2014**, *50*, 8731–8734.
- (50) Hu, Z.; Deibert, B. J.; Li, J. Luminescent Metal–Organic Frameworks for Chemical Sensing and Explosive Detection. *Chem. Soc. Rev.* **2014**, *43*, 5815–5840.
- (51) Feng, D.; Gu, Z.-Y.; Li, J.-R.; Jiang, H.-L.; Wei, Z.; Zhou, H.-C. Zirconium-Metalloporphyrin PCN-222: Mesoporous Metal–Organic Frameworks with Ultrahigh Stability as Biomimetic Catalysts. *Angew. Chem., Int. Ed.* **2012**, *51*, 10307–10310.
- (52) Morris, W.; Voloskiy, B.; Demir, S.; Gandara, F.; McGrier, P. L.; Furukawa, H.; Cascio, D.; Stoddart, J. F.; Yaghi, O. M. Synthesis, Structure, and Metalation of Two New Highly Porous Zirconium Metal–Organic Frameworks. *Inorg. Chem.* **2012**, *51*, 6443–6445.
- (53) Chen, Y.; Hoang, T.; Ma, S. Biomimetic Catalysis of a Porous Iron-Based Metal–Metalloporphyrin Framework. *Inorg. Chem.* **2012**, *51*, 12600–12602.
- (54) Gao, W.-Y.; Chrzanowski, M.; Ma, S. Metal-metalloporphyrin Frameworks: A Resurging Class of Functional Materials. *Chem. Soc. Rev.* **2014**, *43*, 5841–5866.
- (55) Son, H.-J.; Jin, S.; Patwardhan, S.; Wezenberg, S. J.; Jeong, N. C.; So, M.; Wilmer, C. E.; Sarjeant, A. A.; Schatz, G. C.; Snurr, R. Q.; Farha, O. K.; Wiederrecht, G. P.; Hupp, J. T. Light-Harvesting and Ultrafast Energy Migration in Porphyrin-Based Metal–Organic Frameworks. *J. Am. Chem. Soc.* **2013**, *135*, 862–869.

(56) Feng, D.; Chung, W.-C.; Wei, Z.; Gu, Z.-Y.; Jiang, H.-L.; Chen, Y.-P.; Darensbourg, D. J.; Zhou, H.-C. Construction of Ultrastable Porphyrin Zr Metal–Organic Frameworks through Linker Elimination. *J. Am. Chem. Soc.* **2013**, *135*, 17105–17110.

(57) Zhao, M.; Ou, S.; Wu, C.-D. Porous Metal–Organic Frameworks for Heterogeneous Biomimetic Catalysis. *Acc. Chem. Res.* **2014**, *47*, 1199–1207.

(58) Zheng, J.; Wu, M.; Jiang, F.; Su, W.; Hong, M. Stable Porphyrin Zr and Hf Metal–Organic Frameworks Featuring 2.5 nm Cages: High Surface Areas, SCSC Transformations and Catalyses. *Chem. Sci.* **2015**, *6*, 3466–3470.

(59) Xu, H.-Q.; Hu, J.; Wang, D.; Li, Z.; Zhang, Q.; Luo, Y.; Yu, S.-H.; Jiang, H.-L. Visible-Light Photoreduction of CO₂ in a Metal–Organic Framework: Boosting Electron–Hole Separation via Electron Trap States. *J. Am. Chem. Soc.* **2015**, *137*, 13440–13443.

(60) Xu, H.-Q.; Wang, K.; Ding, M.; Feng, D.; Jiang, H.-L.; Zhou, H.-C. Seed-Mediated Synthesis of Metal–Organic Frameworks. *J. Am. Chem. Soc.* **2016**, *138*, 5316–5320.

(61) Wang, X.-S.; Chrzanowski, M.; Wojtas, L.; Chen, Y.-S.; Ma, S. Formation of a Metalloporphyrin-Based Nanoreactor by Postsynthetic Metal–Ion Exchange of a Polyhedral-Cage Containing a Metal–Metalloporphyrin Framework. *Chem. - Eur. J.* **2013**, *19*, 3297–3301.

(62) Jiang, H.-L.; Liu, B.; Akita, T.; Haruta, M.; Sakurai, H.; Xu, Q. Au@ZIF-8: CO Oxidation over Gold Nanoparticles Deposited to Metal–Organic Framework. *J. Am. Chem. Soc.* **2009**, *131*, 11302–11303.

(63) Lu, G.; Li, S.; Guo, Z.; Farha, O. K.; Hauser, B. G.; Qi, X.; Wang, Y.; Wang, X.; Han, S.; Liu, X.; DuChene, J. S.; Zhang, H.; Zhang, Q.; Chen, X.; Ma, J.; Loo, S. C. J.; Wei, W. D.; Yang, Y.; Hupp, T. J.; Huo, F. Imparting Functionality to A Metal–Organic Framework Material by Controlled Nanoparticle Encapsulation. *Nat. Chem.* **2012**, *4*, 310–316.

(64) Kuo, C. H.; Tang, Y.; Chou, L. Y.; Sneed, B. T.; Brodsky, C. N.; Zhao, Z. P.; Tsung, C.-K. Yolk–Shell Nanocrystal@ZIF-8 Nanostructures for Gas-Phase Heterogeneous Catalysis with Selectivity Control. *J. Am. Chem. Soc.* **2012**, *134*, 14345–14348.

(65) Li, X.; Guo, Z.; Xiao, C.; Goh, T. W.; Tesfagaber, D.; Huang, W. Tandem Catalysis by Palladium Nanoclusters Encapsulated in Metal–Organic Frameworks. *ACS Catal.* **2014**, *4*, 3490–3497.

(66) Yang, Q.; Xu, Q.; Yu, S.-H.; Jiang, H.-L. Pd Nanocubes@ZIF-8: Integration of Plasmon-Driven Photothermal Conversion with a Metal–Organic Framework for Efficient and Selective Catalysis. *Angew. Chem., Int. Ed.* **2016**, *55*, 3685–3689.

(67) Liu, H.; Chang, L.; Bai, C.; Chen, L.; Luque, R.; Li, Y. Controllable Encapsulation of “Clean” Metal Clusters within MOFs through Kinetic Modulation: Towards Advanced Heterogeneous Nanocatalysts. *Angew. Chem., Int. Ed.* **2016**, *55*, 5019–5023.

(68) Zhu, Q.-L.; Xu, Q. Metal–Organic Framework Composites. *Chem. Soc. Rev.* **2014**, *43*, 5468–5512.